current issues in molecular biology

MDPI

Article

Hesperidin Pretreatment Attenuates Early Intestinal Ischemia/Reperfusion Injury in Rats

Metin Varlı [1,*] and Eda Yıldızhan [2]

[1] Department of General Surgery, Tire State Hospital, İzmir 35900, Türkiye
[2] Department of Histology and Embryology, Recep Tayyip Erdogan University Faculty of Medicine, Rize 53200, Türkiye; edayildizhan21@gmail.com
* Correspondence: drmetinvarli@gmail.com

Abstract

Intestinal ischemia/reperfusion (I/R) injury involves oxidative stress, inflammation, and epithelial damage. This study evaluated the effects of hesperidin (HSP) pretreatment on early intestinal I/R injury in rats. Twenty-eight Wistar albino rats were allocated to control, sham, I/R, and HSP+I/R groups ($n = 7$/group). HSP was administered orally at 100 mg/kg/day for seven days. I/R was induced 24 h after the final dose by superior mesenteric artery occlusion for 30 min followed by 120 min of reperfusion. Assessments included serum biochemical markers, ileal histopathology, cleaved caspase-3 and total NF-κB p65 immunoreactivity, intestinal malondialdehyde (MDA) content, glutathione peroxidase (GPX) and catalase (CAT) activities, and tissue apoptosis-associated proteins. Compared with untreated I/R, the HSP+I/R group had 49.5% lower serum MDA concentrations, lower myeloperoxidase (MPO) concentrations, and higher glutathione peroxidase 1 (GPX1), superoxide dismutase 1 (SOD1), and CAT concentrations (all Games–Howell-adjusted $p < 0.001$). The HSP+I/R group also had lower intestinal MDA content, lower total caspase-3 and Bax concentrations, a lower Bax/Bcl-2 ratio, higher GPX and CAT activities, higher Bcl-2 concentrations, and lower cleaved caspase-3 and total NF-κB p65 immunoreactivity than the untreated I/R group. The intestinal biochemical and immunoreactivity measures in the HSP+I/R group remained different from the corresponding values in both the control and sham groups. HSP pretreatment was associated with attenuation of early intestinal injury, without establishing direct molecular target inhibition, a definitive mechanism, or clinical therapeutic efficacy.

Keywords: hesperidin; intestinal ischemia/reperfusion; lipid peroxidation; antioxidant enzyme activity; apoptosis; Bax/Bcl-2 ratio; NF-κB

Check for updates

Academic Editor: Julius Liobikas

Received: 2 November 2026
Revised: 20 November 2026
Accepted: 21 November 2026
Published: 27 November 2026

Copyright: © 2026 by the authors. Licensee MDPI, Basel, Switzerland. This article is an open access article distributed under the terms and conditions of the Creative Commons Attribution (CC BY) license.

1. Introduction

Ischemia results from insufficient tissue perfusion, leading to oxygen and nutrient deprivation, cellular dysfunction, and potentially irreversible injury [1]. Although restoration of blood flow is essential for tissue survival, reperfusion can exacerbate the initial damage. Ischemia/reperfusion (I/R) injury involves interacting metabolic, oxidative, and inflammatory processes. During ischemia, oxygen deprivation promotes lactate accumulation, intracellular acidosis, and disruption of ion homeostasis. Subsequent reoxygenation can increase reactive oxygen species (ROS) production, amplify inflammatory responses, and trigger cell death, further compromising tissue integrity [1–3].

The intestine is particularly vulnerable to I/R injury. Acute interruption of superior mesenteric artery (SMA) blood flow can cause epithelial disruption, villus damage, and

progressive mucosal necrosis [4,5]. Acute mesenteric ischemia therefore remains a serious clinical condition associated with substantial morbidity and mortality despite advances in diagnosis and treatment [6–8]. Strategies that preserve intestinal structure and attenuate reperfusion-associated injury remain an important area of experimental investigation.

Oxidative stress and inflammation are closely interconnected components of intestinal I/R injury [9]. Excessive ROS production promotes lipid peroxidation and damage to cellular macromolecules, while impaired antioxidant defenses increase tissue susceptibility to injury [10]. Neutrophil accumulation and inflammatory signaling involving nuclear factor kappa B (NF-κB) can further amplify mucosal damage [9,11]. Alongside these processes, assessment of apoptosis-associated changes can provide a complementary measure of tissue injury. Evaluating oxidative stress, inflammatory markers, and cleaved caspase-3 and NF-κB p65 immunoreactivity together may therefore provide a more comprehensive characterization of the intestinal response to I/R [12].

Hesperidin (HSP) is a flavanone glycoside abundant in citrus fruits, particularly oranges and lemons [13]. Its antioxidant, anti-inflammatory, and cytoprotective properties have been reported in experimental models of tissue injury [14]. Previous studies suggest that HSP can reduce lipid peroxidation, support endogenous antioxidant defenses, and modulate NF-κB-associated inflammatory responses [15,16]. These properties provide a rationale for investigating HSP pretreatment as a strategy to limit intestinal I/R injury. Integrating tissue morphology with serum biochemical measurements and immunohistochemical assessment may help characterize the effects of HSP pretreatment on intestinal I/R injury [17].

Although previous studies have reported protective effects of hesperidin in experimental I/R models, further characterization of local intestinal biochemical changes alongside mucosal morphology and injury-associated immunoreactivity remains useful. We hypothesized that oral HSP pretreatment would attenuate early intestinal I/R injury, accompanied by lower intestinal lipid peroxidation, preservation of antioxidant enzyme activities, and less pronounced apoptosis-associated changes. Accordingly, this study combined ileal histopathology and serum biochemical measurements with intestinal MDA content, GPX and CAT activities, total caspase-3, Bax and Bcl-2 concentrations, the Bax/Bcl-2 ratio, and cleaved caspase-3 and total NF-κB p65 immunoreactivity. The experimental contribution lies in evaluating these complementary outcomes within the same intestinal I/R model.

2. Materials and Methods

2.1. Ethical Approval and Animal Welfare

All procedures were approved by the Dicle University Animal Experiments Ethics Committee (Protocol No. 2025/29; 25 December 2025) and conducted in accordance with the Guide for the Care and Use of Laboratory Animals [18]. Twenty-eight Wistar albino rats aged 8–10 weeks and weighing 200–250 g were housed at 22 ± 3 °C under a 12 h light/dark cycle, with free access to chow and water except during preoperative fasting. An a priori G*Power v3.1.9.4 analysis (Heinrich Heine University, Düsseldorf, Germany; one-way ANOVA, four groups, $f = 0.70$, $\alpha = 0.05$, 80% power) supported the inclusion of 28 animals.

2.2. Hesperidin Pretreatment and Group Allocation

Hesperidin (HSP; ≥97% purity; Sigma-Aldrich, St. Louis, MO, USA) was administered by oral gavage at 100 mg/kg/day for seven consecutive days, at approximately the same time each day. The dose was informed by previous experimental studies [19,20]. Hesperidin was prepared in physiological saline for oral gavage. The amount administered was individually adjusted according to each animal's body weight to deliver 100 mg/kg/day. The 24 h interval

between the final dose and I/R induction was a fixed feature of the prophylactic protocol, rather than a pharmacokinetically validated optimal interval.

An animal caretaker who was not involved in the experimental procedures and was unaware of the planned interventions allocated the rats to four groups ($n = 7$/group):

- Control: Physiological saline (1 mL/day by oral gavage for seven days), without surgical intervention.
- Sham: Physiological saline (1 mL/day by oral gavage for seven days), followed by laparotomy and superior mesenteric artery (SMA) exposure without occlusion; anesthesia duration matched the I/R procedure.
- I/R: The same saline regimen, followed by SMA occlusion for 30 min and reperfusion for 120 min.
- HSP+I/R: HSP pretreatment followed by the same I/R procedure, initiated 24 h after the final dose.

The surgeon was aware of group allocation. Samples were labeled with numerical identifiers (1–28) without group information; biochemical analyses, histopathological assessments, and digital immunohistochemical quantification were performed blinded to group allocation.

2.3. Intestinal I/R and Sample Collection

After 12 h of fasting with water available, anesthesia was induced using intraperitoneal ketamine (90 mg/kg) and xylazine (10 mg/kg). Anesthetic depth was assessed by the absence of a withdrawal response to toe pinch, and body temperature was measured using a digital rodent thermometer (BIO-TK8851; Bioseb). No perioperative fluids were administered, and no additional physiological monitoring was performed.

Under aseptic conditions, the abdomen was disinfected with 10% povidone–iodine and opened by midline laparotomy. The intestinal loops were handled with saline-moistened gauze, and an atraumatic clamp was placed near the SMA origin. Loss of mesenteric pulsation and intestinal pallor confirmed ischemia. After 30 min, the clamp was removed; return of pulsation and coloration confirmed reperfusion, which continued for 120 min [21,22]. Animals remained under anesthesia throughout surgery and the 120-min reperfusion period and were not allowed to recover consciousness. Anesthetic depth was monitored by the absence of a withdrawal response to toe pinch. No separate analgesic was administered. At the planned endpoint, blood was collected by cardiac puncture under deep anesthesia, followed by euthanasia by exsanguination. No animal required early euthanasia.

Immediately after completion of the 120 min reperfusion period, blood was collected by cardiac puncture under deep anesthesia. Serum was separated by centrifugation at 3000 rpm for 10 min at room temperature and stored at −80 °C until analysis. An approximately 2 cm terminal ileum segment was sampled approximately 10 cm proximal to the ileocecal junction. Tissue for morphology was fixed in 10% neutral-buffered formalin; tissue for biochemical analysis was rinsed in cold saline, blotted dry, weighed, and stored at −80 °C.

2.4. Biochemical Analyses

2.4.1. Serum Biochemical Measurements

Rat-specific ELISAs (Bioassay Technology Laboratory, Shanghai, China) quantified MDA, GPX1, SOD1, CAT and MPO [23–25]. Catalog numbers and manufacturer-reported assay ranges were: MDA, E0156Ra, 0.05–10 nmol/mL; GPX1, E1172Ra, 0.5–200 ng/mL; SOD1, E1444Ra, 0.05–30 ng/mL; CAT, E0869Ra, 1–300 ng/mL; and MPO, E0574Ra, 0.5–100 ng/mL.

All serum ELISA measurements were repeated using undiluted samples (dilution factor = 1). Standards and samples were analyzed in duplicate. Plates were washed

using an ELx50 washer and read using an ELx800 reader (BioTek Instruments Inc., Winooski, VT, USA); concentrations were calculated from the corresponding standard curves. Serum GPX1, SOD1, CAT, and MPO results represent concentrations (ng/mL), not enzyme activities.

Manufacturer-reported sensitivities for MDA, GPX1, SOD1, and CAT were 0.01 nmol/mL, 0.23 ng/mL, 0.024 ng/mL, and 0.52 ng/mL, respectively. Corresponding intra-assay CV ranges across three manufacturer test samples were 3.4–5.0%, 3.3–5.7%, 3.2–4.9%, and 5.3–7.4%; inter-assay CVs were <10% for these four kits. These are manufacturer specifications rather than study-specific precision estimates.

2.4.2. Tissue Lipid Peroxidation and Antioxidant Activities

Tissues were homogenized on ice in phosphate-buffered saline (0.01 M, pH 7.4; 1 g tissue:9 mL buffer) and centrifuged at 10,000 × g for 30 min at 4 °C. Supernatants were aliquoted and stored at −80 °C, avoiding repeated freeze–thaw cycles. Total protein was measured using the Bradford method.

Elabscience colorimetric kits measured MDA by the thiobarbituric acid method at 532 nm (E-BC-K025-S), GPX activity by glutathione consumption using 5,5′-dithiobis-(2-nitrobenzoic acid) (DTNB) at 412 nm (E-BC-K096-M), and CAT activity by residual hydrogen peroxide–molybdate complex formation at 405 nm (E-BC-K031-M). GPX measurements were corrected for nonenzymatic glutathione oxidation. Dilutions were selected by preliminary testing to keep measurements within assay ranges. MDA was expressed as nmol/mg protein; GPX and CAT activities were expressed as U/mg protein.

2.4.3. Tissue Apoptosis-Associated Proteins

Total caspase-3, Bax, and Bcl-2 were measured using rat-specific sandwich ELISAs (Elabscience; E-EL-R0160, E-EL-R0098, and E-EL-R0096, respectively). Standards and samples were analyzed in duplicate (100 µL/well) according to the kit protocols, with absorbance measured at 450 nm after reaction termination. Concentrations were derived from standard curves, corrected for dilution, and normalized to total protein (ng/mg protein). The dimensionless Bax/Bcl-2 ratio was calculated separately for each animal. Tissue total caspase-3 was distinguished from cleaved caspase-3 immunoreactivity.

2.5. Histopathology

Ileal samples were fixed for at least 24 h, embedded in paraffin, sectioned at 4–5 µm, and stained with hematoxylin and eosin. Mucosal injury was graded using the Chiu scale (0–5). Inflammatory infiltration and vascular congestion were each scored on a scale of 0–3. Two observers independently scored three microscopic fields in one ileal section per animal and were blinded to group allocation and to each other's ratings. For each outcome, each observer's section-level score was calculated as the mean of the three field scores. The two observers' section-level scores were then averaged to obtain the animal-level value used in the statistical analysis. Interobserver reliability was assessed using a two-way random-effects intraclass correlation coefficient for single measurements with absolute agreement [ICC(2,1)].

2.6. Immunohistochemistry and Digital H-Scoring

Sections were deparaffinized and rehydrated, treated with 3% hydrogen peroxide to block endogenous peroxidase, and subjected to nonspecific binding blockade. Primary antibodies were NF-κB p65 (sc-8008) and cleaved caspase-3 (sc-22171-R), both at 1:120 (Santa Cruz Biotechnology, Dallas, TX, USA). Staining was visualized with DAB and hematoxylin counterstaining.

For each antibody, all groups were processed in the same staining run. Images were acquired using ZEISS ZEN lite 3.12, with identical exposure, illumination, white-balance, and RGB settings. Randomly selected, nonoverlapping fields were analyzed in QuPath by a blinded researcher. Brightfield (H-DAB) image type and default stain vectors were used.

Positive cell detection used the Hematoxylin OD channel, a background radius of 15 pixels, median filter radius of 0 pixels, sigma of 3 pixels, nuclear area limits of 10–1000 pixels^2, detection threshold of 0.1, maximum background intensity of 2, and cell expansion of 5 pixels. Default DAB OD thresholds classified staining as negative (<0.2), weak (0.2 to <0.4), moderate (0.4 to <0.6), or strong (≥0.6); the same settings were used for all groups and sections. Nuclear and cytoplasmic staining were quantified separately using the "Nucleus: DAB OD mean" and "Cytoplasm: DAB OD mean" measurements, respectively. An H-score was calculated for each compartment as (1 × percentage weak) + (2 × percentage moderate) + (3 × percentage strong) [26]. The final image-level score was calculated as the arithmetic mean of the nuclear and cytoplasmic H-scores, retaining a range of 0–300. For NF-κB p65, "total" refers to the protein detected rather than combined nuclear and cytoplasmic staining. Nuclear p65 immunoreactivity alone was not considered evidence of nuclear translocation or pathway activation.

2.7. Statistical Analysis

Analyses used IBM SPSS Statistics v25.0 (IBM Corp., Armonk, NY, USA). Each animal was treated as an independent experimental unit. Continuous outcomes are presented as mean ± standard deviation (SD), and ordinal histopathological scores are presented as median (minimum–maximum). Continuous outcomes were analyzed using Welch's ANOVA followed by Games–Howell pairwise comparisons. Ordinal outcomes were analyzed using the Kruskal–Wallis test followed by two-sided exact permutation Mann–Whitney tests with Holm adjustment. For both procedures, multiplicity adjustment covered all six pairwise group comparisons within each outcome. Omnibus p values were unadjusted across outcomes. Pairwise comparisons were considered statistically significant at an adjusted $p < 0.05$. For HSP+I/R versus I/R, continuous outcomes were reported as mean differences with simultaneous 95% Games–Howell confidence intervals and percentage differences in arithmetic means. Ordinal outcomes were reported as differences in group medians and rank-biserial correlations.

Sensitivity analyses examined the HSP+I/R versus I/R contrast across five serum outcomes, two immunohistochemical H-scores, and three histopathological scores. On the original scale, Welch's t-tests were used for the seven continuous outcomes and two-sided exact permutation Mann–Whitney tests for the three ordinal outcomes, with Holm adjustment across all ten comparisons. The seven continuous outcomes were also analyzed using Welch's t-tests after natural-log transformation, with Holm adjustment across those seven comparisons. A separate rank-based analysis used two-sided exact permutation Mann–Whitney tests for all ten outcomes, with Holm adjustment across the ten comparisons. These analyses are summarized in Supplementary Table S5. Tissue biochemical outcomes were analyzed separately.

3. Results

3.1. Hesperidin Pretreatment Attenuates Serum Biochemical Alterations After Intestinal I/R

Serum concentrations of MDA, GPX1, SOD1, CAT, and MPO differed among the four groups (Welch's ANOVA, all $p < 0.001$, Table S1). Compared with the sham group, the I/R group had higher MDA and MPO concentrations and lower GPX1, SOD1, and CAT concentrations (all Games–Howell-adjusted $p < 0.001$).

Compared with untreated I/R, the HSP+I/R group had 49.5% lower MDA and 45.2% lower MPO concentrations, along with 88.3% higher GPX1, 94.9% higher SOD1, and 65.6% higher CAT concentrations (all Games–Howell-adjusted $p < 0.001$, Figure 1A–E). Concentrations of all five markers in the HSP+I/R group remained significantly different from those in both the control and sham groups (all Games–Howell-adjusted $p < 0.05$). Treatment effect estimates and full pairwise comparisons are reported in Table S3 and Table S6, respectively.

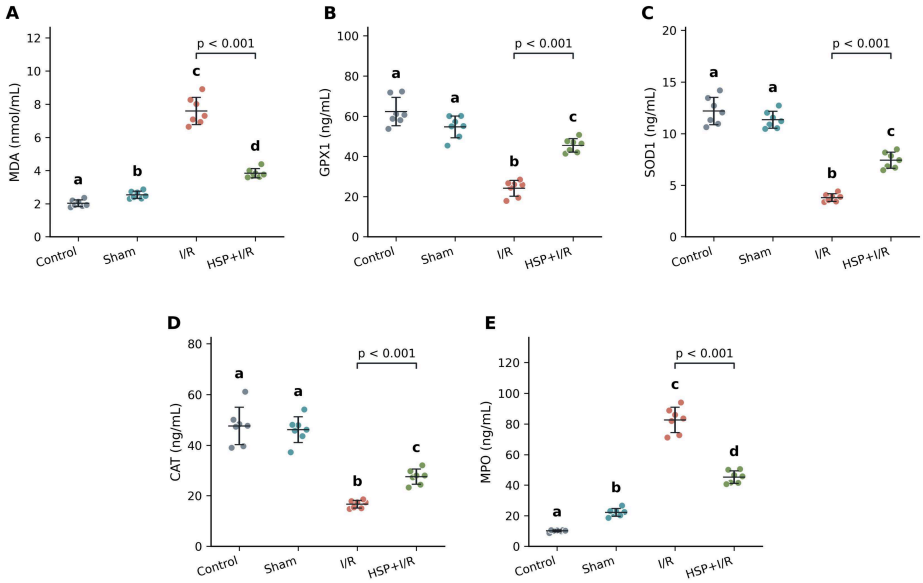


Figure 1. Serum biochemical markers after intestinal ischemia/reperfusion (I/R). (**A**) Malondialdehyde (MDA), (**B**) glutathione peroxidase 1 (GPX1), (**C**) superoxide dismutase 1 (SOD1), (**D**) catalase (CAT), and (**E**) myeloperoxidase (MPO). Each point represents one animal ($n = 7$ per group). Horizontal lines show group means, and error bars indicate standard deviations. Within each panel, groups with no letter in common differ significantly (Games–Howell-adjusted $p < 0.05$ following Welch's ANOVA). Brackets show the adjusted p values for the comparison between the untreated I/R and hesperidin-pretreated I/R (HSP+I/R) groups.

3.2. Hesperidin Pretreatment Attenuates Intestinal Mucosal Injury

H&E-stained sections from the control and sham groups showed generally preserved villus architecture and epithelial continuity. The I/R group exhibited villus-tip epithelial disruption, sloughing, distortion of mucosal architecture, and vascular congestion. In HSP+I/R, villus structure and epithelial continuity were better preserved, although focal surface irregularities and residual epithelial alterations remained (Figure 2).

Histopathological scores differed among groups (Kruskal–Wallis test, all $p < 0.001$; Table 1). Median mucosal injury scores were 5.0 (4.5–5.0) in I/R and 1.0 (0.5–1.5) in HSP+I/R. Median inflammatory infiltration and vascular congestion scores were both 3.0 in I/R and 1.0 in HSP+I/R. All three scores were lower following HSP pretreatment (Holm-adjusted $p = 0.0035$ for each comparison; Figure S1, panels A–C). Compared with sham, HSP+I/R retained higher mucosal injury and inflammatory infiltration scores (adjusted $p = 0.0256$ and 0.0070, respectively), whereas vascular congestion did not differ significantly (adjusted $p = 0.0559$). Interobserver reliability estimates were 0.89 (95% CI: 0.80–0.92) for mucosal injury, 0.92 (95% CI: 0.90–0.94) for inflammatory infiltration, and 0.92 (95% CI: 0.89–0.96) for vascular congestion. Table S4 reports the histopathological score distributions and effect estimates. Table S7 reports the adjusted p values for all pairwise comparisons.

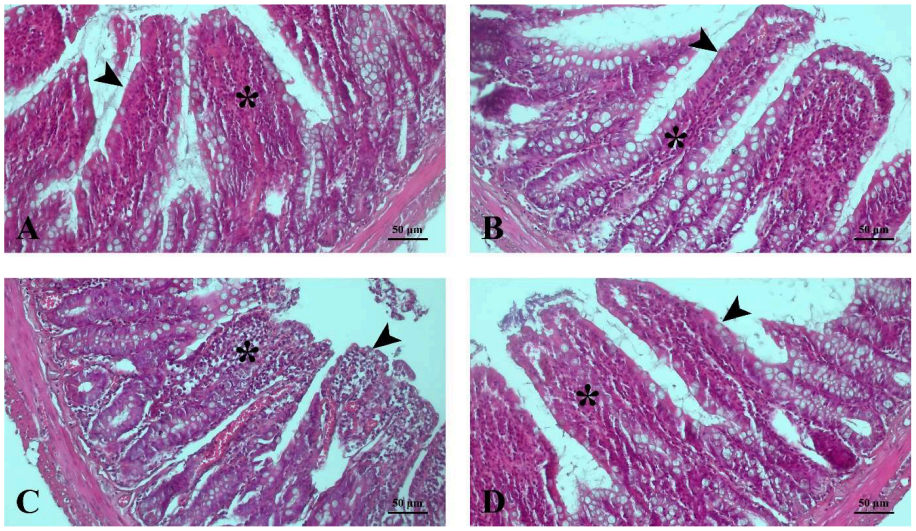


Figure 2. Representative H&E-stained ileal sections. (**A**) Control and (**B**) Sham: generally preserved mucosal architecture. (**C**) I/R: villus-tip epithelial disruption and sloughing, with vascular congestion in the lamina propria. (**D**) HSP+I/R: relatively preserved villus architecture with residual focal epithelial alterations. Arrowheads: epithelium; asterisks (*): lamina propria. Scale bars: 50 µm. HSP, hesperidin; I/R, ischemia/reperfusion.

Table 1. Intestinal histopathological scores in the experimental groups.

Parameter	Control ($n = 7$)	Sham ($n = 7$)	I/R ($n = 7$)	HSP+I/R ($n = 7$)	Overall p	Adjusted p, I/R vs. HSP+I/R
Mucosal injury (0–5)	0.0 (0.0–0.5)	0.0 (0.0–1.0)	5.0 (4.5–5.0)	1.0 (0.5–1.5)	<0.001	0.0035
Inflammatory infiltration (0–3)	0.0 (0.0–0.0)	0.0 (0.0–0.5)	3.0 (2.5–3.0)	1.0 (0.5–1.5)	<0.001	0.0035
Vascular congestion (0–3)	0.0 (0.0–1.0)	0.0 (0.0–1.0)	3.0 (2.0–3.0)	1.0 (0.5–1.5)	<0.001	0.0035

Values are median (minimum–maximum); $n = 7$ per group. Each animal-level score is the arithmetic mean of two observers' independent ratings. Overall comparisons used Kruskal–Wallis tests, followed by two-sided exact permutation Mann–Whitney comparisons with Holm adjustment across six pairs within each outcome. The final column shows I/R versus HSP+I/R.

3.3. Hesperidin Pretreatment Reduces Cleaved Caspase-3 Immunoreactivity

Control and sham sections showed predominantly faint cytoplasmic cleaved caspase-3 staining along the villus and crypt epithelium, with scattered brown DAB positivity in lamina propria cells. In I/R, staining was more extensive and conspicuous in villus epithelial cells and the underlying lamina propria, including regions with irregular villus surfaces and epithelial detachment. HSP+I/R showed less intense and less extensive staining along relatively preserved epithelial profiles, although focal positivity remained in the epithelium and lamina propria (Figure 3).

H-scores differed among groups (Welch ANOVA, $p < 0.001$; Table 2). HSP+I/R had a lower mean H-score than I/R (65.29 ± 6.32 vs. 182.71 ± 34.10; Games–Howell-adjusted $p < 0.001$), but remained above sham (30.00 ± 5.48; adjusted $p < 0.001$; Figure S1, panel D).

3.4. Hesperidin Pretreatment Reduces Total NF-κB p65 Immunoreactivity

Control and sham sections exhibited heterogeneous NF-κB p65 staining, with faint-to-moderate brown DAB immunoreactivity along villus and crypt epithelial profiles and focal positivity among lamina propria cells. In I/R, more conspicuous staining involved several villus epithelial profiles and the cellular cores of the villi, with regional variation in intensity. HSP+I/R showed predominantly faint-to-moderate epithelial staining, with

residual focal positivity in the lamina propria and around some crypt profiles. The epithelial lining appeared relatively preserved compared with untreated I/R (Figure 4).

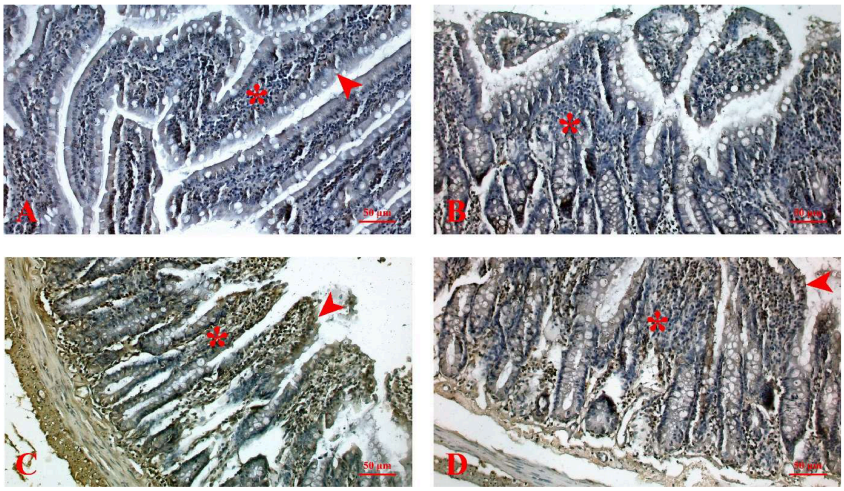


Figure 3. Representative cleaved caspase-3 immunostaining in ileal sections. (**A**) Control and (**B**) Sham: predominantly faint staining in the villus and crypt epithelium, with focal lamina propria positivity. (**C**) I/R: more extensive brown DAB immunoreactivity in epithelial and lamina propria compartments. (**D**) HSP+I/R: less extensive and less intense staining with residual focal positivity. Brown indicates DAB immunoreactivity; blue indicates hematoxylin counterstaining. Arrowheads: epithelium; asterisks (*): lamina propria. Scale bars: 50 µm. HSP, hesperidin; I/R, ischemia/reperfusion.

Total p65 H-scores differed among groups (Welch ANOVA, $p < 0.001$; Table 2). HSP+I/R had a lower mean H-score than I/R (66.43 ± 10.44 vs. 188.86 ± 35.37; Games–Howell-adjusted $p < 0.001$), but remained above sham (19.57 ± 4.50; adjusted $p < 0.001$; Figure S1, panel E).

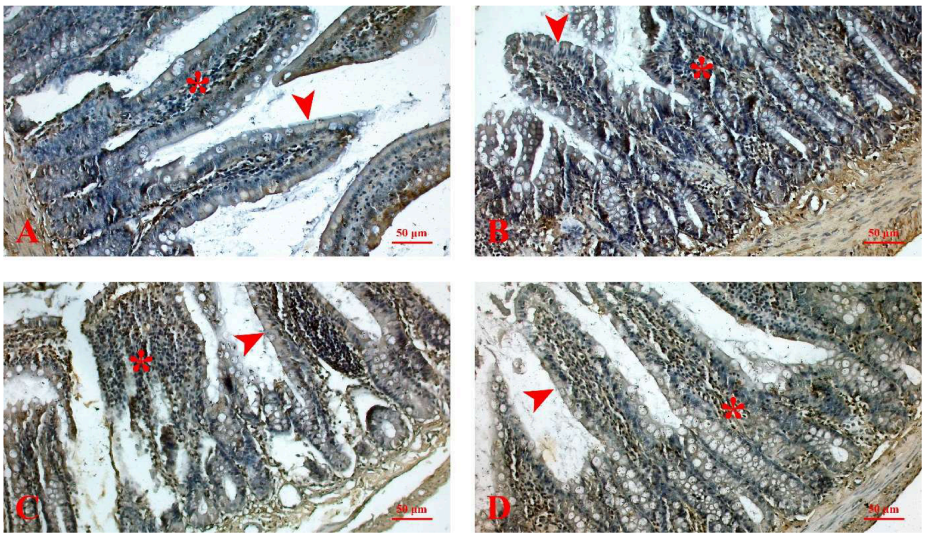


Figure 4. Representative NF-κB p65 immunostaining in ileal sections. (**A**) Control and (**B**) Sham: heterogeneous epithelial and lamina propria brown DAB staining. (**C**) I/R: more conspicuous brown DAB immunoreactivity in villus epithelial profiles and lamina propria cells. (**D**) HSP+I/R: predominantly faint-to-moderate epithelial staining with residual focal lamina propria and crypt-associated positivity. Brown indicates DAB immunoreactivity; blue indicates hematoxylin counterstaining. Arrowheads: epithelium; asterisks (*): lamina propria. Scale bars: 50 µm. HSP, hesperidin; I/R, ischemia/reperfusion.

Table 2. Intestinal cleaved caspase-3 and total NF-κB p65 H-scores.

Parameter	Control ($n = 7$)	Sham ($n = 7$)	I/R ($n = 7$)	HSP+I/R ($n = 7$)	Overall p	Adjusted p, I/R vs. HSP+I/R
Cleaved caspase-3 H-score	19.86 ± 5.55	30.00 ± 5.48	182.71 ± 34.10	65.29 ± 6.32	<0.001	<0.001
NF-κB p65 H-score	13.43 ± 3.46	19.57 ± 4.50	188.86 ± 35.37	66.43 ± 10.44	<0.001	<0.001

Values are mean ± standard deviation; $n = 7$ per group. H-scores range from 0 to 300. Overall comparisons used Welch ANOVA, followed by Games–Howell comparisons across six pairs within each marker. The final column shows I/R versus HSP+I/R. NF-κB, nuclear factor kappa B.

3.5. Hesperidin Pretreatment Attenuates Intestinal Lipid Peroxidation and Preserves Antioxidant Enzyme Activities

Intestinal MDA content and GPX and CAT activities differed among groups (Welch ANOVA, all $p < 0.001$; Table S2). Control and sham did not differ significantly. Compared with both groups, I/R had higher MDA content and lower GPX and CAT activities (all Games–Howell-adjusted $p < 0.05$).

Compared with I/R, HSP+I/R had lower MDA content (2.732 ± 0.449 vs. 4.828 ± 0.726 nmol/mg protein; adjusted $p < 0.001$; Figure 5A), higher GPX activity (47.186 ± 6.780 vs. 29.446 ± 2.691 U/mg protein; adjusted $p = 0.0010$; Figure 5B), and higher CAT activity (49.847 ± 6.255 vs. 30.517 ± 3.148 U/mg protein; adjusted $p < 0.001$; Figure 5C). All three measurements remained different from both control and sham values (all adjusted $p < 0.05$). Treatment contrasts and full pairwise comparisons are provided in Tables S3 and S6.

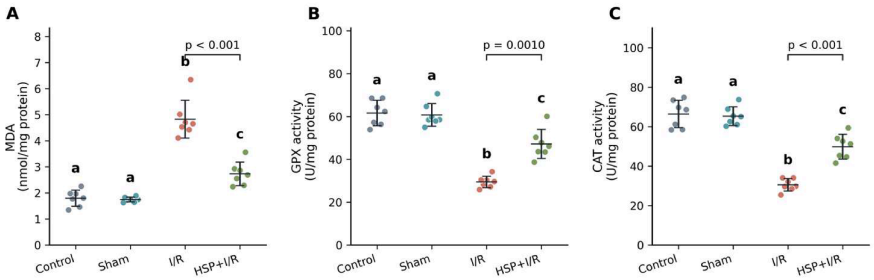


Figure 5. Intestinal lipid peroxidation and antioxidant enzyme activities. (**A**) MDA content, (**B**) GPX activity, and (**C**) CAT activity. Each point represents one animal ($n = 7$ per group); horizontal lines and error bars indicate means and standard deviations. Within each panel, groups sharing a letter do not differ significantly, whereas groups with no shared letter differ at Games–Howell-adjusted $p < 0.05$ following Welch ANOVA. Brackets show adjusted I/R versus HSP+I/R comparisons. MDA, malondialdehyde; GPX, glutathione peroxidase; CAT, catalase; HSP, hesperidin; I/R, ischemia/reperfusion.

3.6. Hesperidin Pretreatment Alters Intestinal Apoptosis-Associated Protein Profiles

Intestinal total caspase-3, Bax, and Bcl-2 concentrations and the Bax/Bcl-2 ratio differed among groups (Welch ANOVA, all $p < 0.001$; Table S2). Control and sham did not differ significantly. Compared with both groups, I/R showed higher total caspase-3 and Bax concentrations and a higher Bax/Bcl-2 ratio, together with lower Bcl-2 concentrations (all Games–Howell-adjusted $p < 0.05$).

Compared with I/R, HSP+I/R had lower total caspase-3 (1.978 ± 0.296 vs. 4.748 ± 0.732 ng/mg protein; Figure 6A) and Bax concentrations (1.680 ± 0.195 vs. 3.356 ± 0.271 ng/mg protein; Figure 6B), higher Bcl-2 concentrations (1.872 ± 0.259 vs. 0.985 ± 0.124 ng/mg protein; Figure 6C), and a lower Bax/Bcl-2 ratio (0.903 ± 0.084 vs. 3.429 ± 0.271; Figure 6D; all adjusted $p < 0.001$). These measurements remained significantly different from both control and sham values (all adjusted $p < 0.05$; Tables S3 and S6).

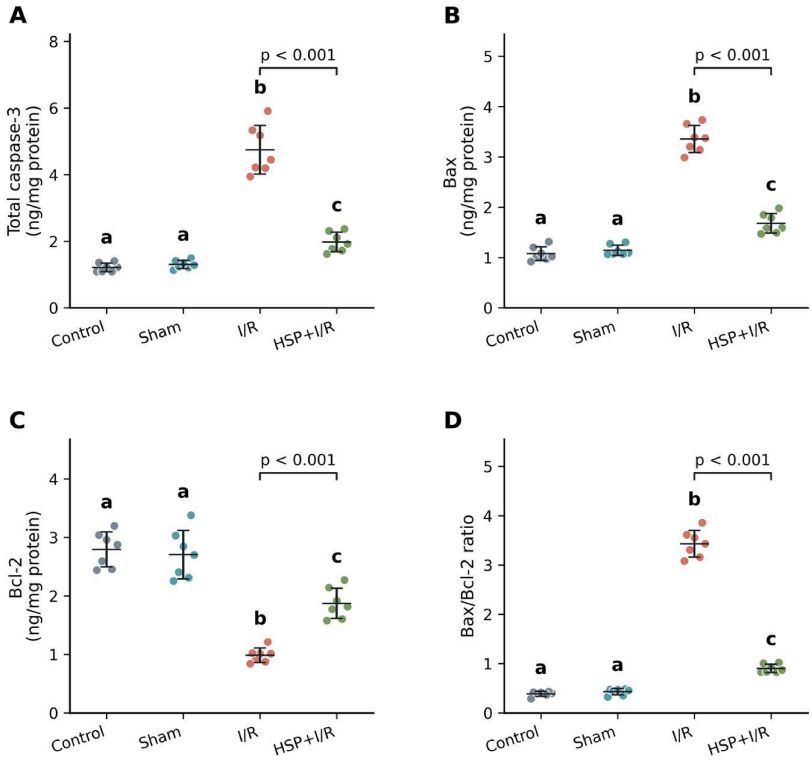


Figure 6. Intestinal apoptosis-associated protein profiles. (**A**) Total caspase-3, (**B**) Bax, (**C**) Bcl-2, and (**D**) Bax/Bcl-2 ratio. Each point represents one animal ($n = 7$ per group); horizontal lines and error bars indicate means and standard deviations. Within each panel, groups sharing a letter do not differ significantly, whereas groups with no shared letter differ at Games–Howell-adjusted $p < 0.05$ following Welch ANOVA. Brackets show adjusted I/R versus HSP+I/R comparisons. Tissue total caspase-3 measured by ELISA is distinct from the cleaved caspase-3 immunohistochemical endpoint. HSP, hesperidin; I/R, ischemia/reperfusion.

3.7. Exploratory Sensitivity Analyses

The HSP+I/R versus I/R comparisons remained significant for all ten outcomes on the original scale (all Holm-adjusted $p < 0.002$) and in the exact rank analysis (Holm-adjusted $p = 0.0058$ for each outcome). Comparisons also remained significant after log transformation for all seven continuous outcomes (all Holm-adjusted $p < 0.001$, Table S5).

4. Discussion

Hesperidin pretreatment was associated with less severe intestinal mucosal injury, attenuation of serum biochemical alterations, and lower cleaved caspase-3 and total NF-κB p65 immunoreactivity during early reperfusion. The additional intestinal measurements showed lower MDA content, higher GPX and CAT activities, and changes in apoptosis-associated protein concentrations compared with untreated I/R. However, these tissue measurements remained different from control and sham values, indicating incomplete protection. Taken together, the findings support an association between repeated HSP pretreatment and attenuation of early intestinal injury without establishing a single underlying mechanism.

Previous experimental studies provide context for these observations. Pehlivan et al. [27] reported reduced intestinal mucosal injury and lower tissue MDA and MPO measurements following diosmin–hesperidin pretreatment. Because the intervention combined two flavonoids, its effects cannot be attributed specifically to hesperidin. Bayomy et al. [21] demonstrated that hesperidin alone attenuated lung injury secondary to intestinal I/R, supporting an effect on remote organ injury. Protective effects have also been reported in gastric

I/R [19]. The present study complements these findings by combining direct intestinal biochemical measurements with ileal morphology and immunohistochemical assessment.

The distinction between circulating protein concentrations and tissue enzyme activities is important when interpreting the antioxidant findings. Serum GPX1, SOD1, and CAT were quantified by ELISA and therefore represent concentrations rather than catalytic activities. These measurements alone cannot establish improved antioxidant function within the intestinal mucosa. In contrast, lower intestinal MDA content together with higher tissue GPX and CAT activities provides direct evidence of differences in local lipid peroxidation and antioxidant enzyme activity. Nevertheless, these findings cannot distinguish direct radical scavenging from preservation of viable tissue, altered enzyme regulation, or other responses to pretreatment.

The apoptosis-associated findings provide a complementary description of tissue injury. HSP-pretreated animals had lower total caspase-3 and Bax concentrations, higher Bcl-2 concentrations, and a lower Bax/Bcl-2 ratio than untreated I/R animals. These changes, together with reduced cleaved caspase-3 immunoreactivity, are consistent with a less pronounced apoptosis-associated injury profile. Total caspase-3 concentration and cleaved caspase-3 immunoreactivity nevertheless represent distinct endpoints, and neither substitutes for a direct caspase activity assay. Similarly, the Bax/Bcl-2 ratio does not independently demonstrate mitochondrial membrane permeabilization or establish a causal apoptotic mechanism. Although apoptosis contributes to epithelial loss after intestinal I/R [28], epithelial restitution also influences recovery [29]. Functional barrier measurements and longer follow-up are therefore needed to determine whether the observed morphological preservation translates into sustained intestinal function.

Exploratory docking scores for hesperidin with human caspase-3 and NF-κB p65 are reported in Table S8. Figure S2 shows the corresponding predicted poses, and Figure S3 presents the STRING functional association network and KEGG enrichment results for seven selected rat proteins.

Total p65 immunoreactivity also requires cautious interpretation. NF-κB has context-dependent roles in intestinal inflammation and epithelial survival. Chen et al. [30] showed that enterocyte-specific IKK-β deletion reduced systemic inflammation while increasing local apoptotic injury following intestinal I/R. Zou et al. [31] likewise reported different consequences of NF-κB inhibition at early and later reperfusion intervals. Thus, reduced p65 staining should not be equated with beneficial inhibition of NF-κB signaling. Because phosphorylation, nuclear translocation, and downstream inflammatory gene expression were not specifically evaluated, the present p65 findings are best interpreted as differences in tissue immunoreactivity associated with the injury response.

Exposure at the time of injury remains another unresolved issue. Human absorption studies emphasize the importance of hesperidin metabolism [32], and rat studies demonstrate circulating conjugated metabolites after oral administration [33]. Previous experimental work supports repeated oral pretreatment, including seven-day regimens [34]. A human intervention study also reported endothelial effects assessed 24 h after the final dose [33], although this provides only indirect context for the present protocol. Neither these studies nor the current findings establish that the selected 24-h interval is optimal for intestinal I/R. Because hesperidin and its metabolites were not measured in plasma or intestinal tissue, the relative contributions of residual exposure, metabolites, and persistent biological responses to repeated administration cannot be distinguished.

Several design and analytical limitations should also be considered. The small group size limits precision, and evaluation of a single dose prevents conclusions about dose dependence or an optimal protective dose. Without an HSP-only group, baseline effects in uninjured animals cannot be separated from effects under I/R conditions. The control,

sham, and I/R groups received the same daily saline gavage regimen to standardize the administration procedure. Limited perioperative physiological monitoring restricts assessment of hemodynamic or respiratory influences. The software-default DAB thresholds were applied consistently but were not independently validated.

Finally, seven days of pretreatment followed by assessment after 120 min of reperfusion represents a prophylactic, early-injury model. It does not establish efficacy when treatment begins after ischemia, demonstrate sustained recovery, or support clinical therapeutic recommendations. Further studies should evaluate dose–response relationships, treatment initiated at or after reperfusion, plasma and tissue exposure, intestinal barrier function, and longer-term outcomes.

5. Conclusions

Hesperidin pretreatment was associated with reduced intestinal histological injury, attenuation of serum biochemical alterations, and lower cleaved caspase-3 and total NF-κB p65 immunoreactivity during the early reperfusion period in rats. These findings support a protective association under the experimental conditions studied but do not establish direct molecular target inhibition, a definitive mechanism of action, or clinical therapeutic efficacy. Further studies incorporating exposure measurements, functional pathway assessments, and longer follow-up are needed to clarify the mechanisms and translational relevance of these observations.

Supplementary Materials: The following supporting information can be downloaded at https://www.mdpi.com/article/10.3390/cimb48121293/s1.

Author Contributions: Conceptualization, M.V.; methodology, M.V. and E.Y.; software, M.V.; validation, M.V. and E.Y.; formal analysis, M.V.; investigation, M.V. and E.Y.; resources, M.V.; data curation, M.V. and E.Y.; writing—original draft preparation, M.V. and E.Y.; writing—review and editing, M.V. and E.Y.; visualization, E.Y.; supervision, M.V.; project administration, M.V.; funding acquisition, M.V. All authors have read and agreed to the published version of the manuscript.

Funding: This research received no external funding.

Institutional Review Board Statement: The animal study protocol was approved by the Dicle University Animal Experiments Ethics Committee (protocol code 2025/29; date of approval: 25 December 2025).

Informed Consent Statement: Not applicable.

Data Availability Statement: Data presented in this study can be obtained from the corresponding author upon request.

Acknowledgments: During the preparation of this manuscript, the authors used ChatGPT 6 sol (OpenAI) to assist with language editing, manuscript organization, and figure preparation. The authors reviewed and verified all resulting text, calculations, and figures and take full responsibility for the content of this publication.

Conflicts of Interest: The authors declare no conflicts of interest.

Abbreviations

The following abbreviations are used in this manuscript:

Abbreviation	Definition
ANOVA	Analysis of variance
Bax	Bcl-2-associated X protein
Bcl-2	B-cell lymphoma 2
Casp3	Caspase-3 (rat gene symbol)

CAT	Catalase
CI	Confidence interval
DAB	3,3′-Diaminobenzidine
DTNB	5,5′-Dithiobis-(2-nitrobenzoic acid)
ELISA	Enzyme-linked immunosorbent assay
GPX	Glutathione peroxidase
GPX1	Glutathione peroxidase 1
H&E	Hematoxylin and eosin
H-DAB	Hematoxylin and 3,3′-diaminobenzidine
H-score	Histological score
HSP	Hesperidin
ICC	Intraclass correlation coefficient
IKK-β	Inhibitor of nuclear factor kappa B kinase subunit beta
I/R	Ischemia/reperfusion
KEGG	Kyoto Encyclopedia of Genes and Genomes
MDA	Malondialdehyde
MPO	Myeloperoxidase
NF-κB	Nuclear factor kappa B
RGB	Red, green, and blue
ROS	Reactive oxygen species
SD	Standard deviation
SMA	Superior mesenteric artery
SOD1	Superoxide dismutase 1
SPSS	Statistical Package for the Social Sciences
TNF	Tumor necrosis factor

References

1. Ayaz, H.; Aşır, F.; Korak, T. Skimmianine Showed Neuroprotection against Cerebral Ischemia/Reperfusion Injury. *Curr. Issues Mol. Biol.* **2024**, *46*, 7373–7385. [CrossRef]
2. Karaaslanlı, A.; Tuncer, M.C.; Aşır, F.; Korak, T. Gallic acid showed neuroprotection against endoplasmic reticulum stress in rats. *Acta Cir. Bras.* **2025**, *40*, e400925. [CrossRef]
3. Aşır, F.; Gökalp Özkorkmaz, E.; Yalçın, M.; Şahin, F.; Korak, T. Skimmianine Pretreatment Attenuates Cerebellar Neuroinflammation and Myelin Injury Following Experimental Cerebral Ischemia–Reperfusion. *Antioxidants* **2026**, *15*, 743. [CrossRef]
4. Rock, P.; Yao, Z. Ischemia reperfusion injury, preconditioning and critical illness. *Curr. Opin. Anaesthesiol.* **2002**, *15*, 139–146. [CrossRef]
5. Bala, M.; Catena, F.; Kashuk, J.; De Simone, B.; Gomes, C.A.; Weber, D.; Sartelli, M.; Coccolini, F.; Kluger, Y.; Abu-Zidan, F.M.; et al. Acute mesenteric ischemia: Updated guidelines of the World Society of Emergency Surgery. *World J. Emerg. Surg.* **2022**, *17*, 54. [CrossRef]
6. Silachev, D.N.; Isaev, N.K.; Pevzner, I.B.; Zorova, L.D.; Stelmashook, E.V.; Novikova, S.V. The mitochondria-targeted antioxidants and remote kidney preconditioning ameliorate brain damage through kidney-to-brain cross talk. *PLoS ONE* **2012**, *7*, e51553. [CrossRef]
7. Bhargava, P.; Verma, V.K.; Malik, S.; Khan, S.I.; Bhatia, J.; Arya, D.S. Hesperidin regresses cardiac hypertrophy by virtue of PPAR-γ agonistic, anti-inflammatory, antiapoptotic, and antioxidant properties. *J. Biochem. Mol. Toxicol.* **2019**, *33*, e22283. [CrossRef]
8. Reintam Blaser, A.; Mändul, M.; Björck, M.; Acosta, S.; Bala, M.; Bodnar, Z.; Casian, D.; Demetrashvili, Z.; D'Oria, M.; Durán Muñoz-Cruzado, V.; et al. Incidence, diagnosis, management and outcome of acute mesenteric ischaemia: A prospective, multicentre observational study (AMESI Study). *Crit. Care* **2024**, *28*, 32. [CrossRef]
9. Deng, F.; Sun, Q.-S.; Xie, S.; Wu, L.; He, S.-Y.; Zhou, B.-W.; Hu, Z.; Lian, W.-Y.; Li, B.-J.; Li, C.; et al. Intestinal Ischemia/Reperfusion Injury: Mechanisms, Diagnosis, and Therapeutic Advances. *Int. J. Biol. Sci.* **2026**, *22*, 4059–4073. [CrossRef]
10. Chen, Y.S.; Tian, H.X.; Rong, D.C.; Wang, L.; Chen, S.; Zeng, J.; Xu, H.; Mei, J.; Wang, L.Y.; Liou, Y.L.; et al. ROS homeostasis in cell fate, pathophysiology, and therapeutic interventions. *Mol. Biomed.* **2025**, *6*, 89. [CrossRef]
11. Liu, S.; Liu, J.; Wang, Y.; Deng, F.; Deng, Z. Oxidative Stress: Signaling Pathways, Biological Functions, and Disease. *MedComm* **2025**, *6*, e70268. [CrossRef]
12. Mederle, A.L.; Lascu, A.; Manzur, A.R.; Caraba, A.; Staicu, R.E.; Noveanu, L.; Aburel, O.M. Oxidative Stress in Inflammatory Bowel Disease: From Redox Dysregulation to Translational Targeting. *Antioxidants* **2026**, *15*, 894. [CrossRef]

13. Ermiş, I.S.; Deveci, E.; Aşır, F. Effects of Quince Gel and Hesperidin Mixture on Experimental Endometriosis. *Molecules* **2023**, *28*, 5945. [CrossRef]
14. Amin, A.R.; Kassab, R.B.; Abdel Moneim, A.E.; Amin, H.K. Comparison Among Garlic, Berberine, Resveratrol, *Hibiscus sabdariffa*, *Genus Zizyphus*, Hesperidin, Red Beetroot, *Catha edulis*, *Portulaca oleracea*, and Mulberry Leaves in the Treatment of Hypertension and Type 2 DM: A Comprehensive Review. *Nat. Prod. Commun.* **2020**, *15*, 1934578X20921623. [CrossRef]
15. Mahmoud, A.M.; Mohammed, H.M.; Khadrawy, S.M.; Galaly, S.R. Hesperidin protects against chemically induced hepatocarcinogenesis via modulation of Nrf2/ARE/HO-1, PPARγ and TGF-β1/Smad3 signaling, and amelioration of oxidative stress and inflammation. *Chem. Biol. Interact.* **2017**, *277*, 146–158. [CrossRef]
16. Pari, L.; Shagirtha, K. Hesperetin protects against oxidative stress related hepatic dysfunction by cadmium in rats. *Exp. Toxicol. Pathol.* **2012**, *64*, 513–520. [CrossRef]
17. Zhao, W.; Hong, W.; Cao, Y. Harnessing hesperidin for brain metabolism: Epigenetic signatures, cellular homeostasis, synaptic function, and neuroprotection in age-related diseases and neurodegenerative diseases. *Front. Nutr.* **2025**, *12*, 1706146. [CrossRef]
18. National Research Council. *Guide for the Care and Use of Laboratory Animals*, 9th ed.; The National Academies Press: Washington, DC, USA, 2011; 246p.
19. Ozyigit, F.; Deger, A.N.; Kocak, F.E.; Ekici, M.F.; Simsek, H.; Arık, O. Protective effects of hesperidin in gastric damage caused by experimental ischemia-reperfusion injury model in rats. *Acta Cir. Bras.* **2024**, *39*, e391124. [CrossRef]
20. Li, S.; Qin, Q.; Luo, D.; Pan, W.; Wei, Y.; Xu, Y.; Zhu, J.; Shang, L. Hesperidin ameliorates liver ischemia/reperfusion injury via activation of the Akt pathway. *Mol. Med. Rep.* **2020**, *22*, 4519–4530. [CrossRef]
21. Bayomy, N.A.; Elshafey, S.H.; ElBakary, R.H.; Abdelaziz, E.Z. Protective effect of hesperidin against lung injury induced by intestinal ischemia/reperfusion in adult albino rats: Histological, immunohistochemical and biochemical study. *Tissue Cell* **2014**, *46*, 304–310. [CrossRef]
22. Grootjans, J.; Lenaerts, K.; Derikx, J.P.; Matthijsen, R.A.; de Bruïne, A.P.; van Bijnen, A.A.; van Dam, R.M.; Dejong, C.H.; Buurman, W.A. Human intestinal ischemia-reperfusion-induced inflammation characterized: Experiences from a new translational model. *Am. J. Pathol.* **2010**, *176*, 2283–2291. [CrossRef]
23. Üstündağ, H.; Demir, Ö.; Çiçek, B.; Huyut, M.T.; Yüce, N.; Tavacı, T. Protective effect of melatonin and ascorbic acid combination on sepsis-induced lung injury: An Experimental study. *Clin. Exp. Pharmacol. Physiol.* **2023**, *50*, 634–646. [CrossRef]
24. Aşır, F.; Aslanoğlu, B.; Tutal Gürsoy, G.; Tuncer, M.C. Resveratrol showed anti-inflammatory effects on hippocampus via suppressing NFκB. *Folia Morphol.* **2024**, *83*, 571–577. [CrossRef]
25. Kabalı, S.; Ünlü Söğüt, M.; Öner, N.; Kara, A. Protective Effects of Propolis Supplementation on Aflatoxin B1-Induced Oxidative Stress, Antioxidant Status, Intestinal Barrier Damage, and Gut Microbiota in Rats. *Mol. Nutr. Food Res.* **2025**, *69*, e70052. [CrossRef]
26. Guler, R.; Ozden, E.; Asır, F.; Gulsun, B. High-Dose Shilajit Enhances Xenograft-Mediated Bone Regeneration in a Rat Tibial Defect Model: An In Vivo Experimental Study. *Life* **2025**, *15*, 1528. [CrossRef]
27. Pehlivan, M.; Hazinedaroglu, S.M.; Kayaoglu, H.A.; Erkek, A.B.; Keklik, T.; Canbolat, O.; Kocak, S. The Effect of Diosmin Hesperidin on Intestinal Ischaemia—Reperfusion Injury. *Acta Chir. Belg.* **2004**, *104*, 715–718. [CrossRef]
28. Ikeda, H.; Suzuki, Y.; Suzuki, M.; Koike, M.; Tamura, J.; Tong, J.; Nomura, M.; Itoh, G. Apoptosis is a major mode of cell death caused by ischaemia and ischaemia/reperfusion injury to the rat intestinal epithelium. *Gut* **1998**, *42*, 530–537. [CrossRef]
29. Grootjans, J.; Thuijls, G.; Derikx, J.P.; van Dam, R.M.; Dejong, C.H.; Buurman, W.A. Rapid lamina propria retraction and zipper-like constriction of the epithelium preserves the epithelial lining in human small intestine exposed to ischaemia-reperfusion. *J. Pathol.* **2011**, *224*, 411–419. [CrossRef]
30. Chen, L.-W.; Egan, L.; Li, Z.-W.; Greten, F.R.; Kagnoff, M.F.; Karin, M. The two faces of IKK and NF-κB inhibition: Prevention of systemic inflammation but increased local injury following intestinal ischemia-reperfusion. *Nat. Med.* **2003**, *9*, 575–581. [CrossRef]
31. Zou, L.; Attuwaybi, B.; Kone, B.C. Effects of NF-kappa B inhibition on mesenteric ischemia-reperfusion injury. *Am. J. Physiol.-Gastrointest. Liver Physiol.* **2003**, *284*, G713–G721. [CrossRef]
32. Actis-Goretta, L.; Dew, T.P.; Lévèques, A.; Pereira-Caro, G.; Rein, M.; Teml, A.; Schäfer, C.; Hofmann, U.; Schwab, M.; Eichelbaum, M.; et al. Gastrointestinal absorption and metabolism of hesperetin-7-O-rutinoside and hesperetin-7-O-glucoside in healthy humans. *Mol. Nutr. Food Res.* **2015**, *59*, 1651–1662. [CrossRef]
33. Nectoux, A.M.; Abe, C.; Huang, S.W.; Ohno, N.; Tabata, J.; Miyata, Y.; Tanaka, K.; Tanaka, T.; Yamamura, H.; Matsui, T. Absorption and Metabolic Behavior of Hesperidin (Rutinosylated Hesperetin) after Single Oral Administration to Sprague-Dawley Rats. *J. Agric. Food Chem.* **2019**, *67*, 9812–9819. [CrossRef]
34. Gaur, V.; Aggarwal, A.; Kumar, A. Possible nitric oxide mechanism in the protective effect of hesperidin against ischemic reperfusion cerebral injury in rats. *Indian J. Exp. Biol.* **2011**, *49*, 609–618.

Disclaimer/Publisher's Note: The statements, opinions and data contained in all publications are solely those of the individual author(s) and contributor(s) and not of MDPI and/or the editor(s). MDPI and/or the editor(s) disclaim responsibility for any injury to people or property resulting from any ideas, methods, instructions or products referred to in the content.